Nanofabrication

DOI: 10.1002/anie.201006991

Gutenberg-Style Printing of Self-Assembled Nanoparticle Arrays: Electrostatic Nanoparticle Immobilization and DNA-Mediated Transfer**

*Yuanhui Zheng, Cecilia H. Lalander, Thibaut Thai, Scott Dhuey, Stefano Cabrini, and Udo Bach**

Nanofabrication tools such as electron beam[1–3] and scanning probe lithography[4–9] can be used to fabricate nanostructures with resolutions well beyond the capability of today's most advanced photolithography tools. A general drawback of these direct-write techniques, however, is their slow writing speed, prohibiting their direct exploitation in commercial fabrication processes. Novel nanoprinting techniques such as microcontact printing (μCP),[10,11] nanoimprinting,[12] and nanostencil lithography[13] could offer a practical solution to this limitation, as they make it possible to replicate these nanostructures in repetitive printing cycles, offering the opportunity to produce complex nanostructures at low cost, with otherwise unmatched resolution capabilities. So far, a number of printing techniques have been developed that exploit the specific affinity of molecular inks to stamp (i.e., print master) and print substrates.[10–15] The self-assembly of alkanethiol monolayers on patterned poly(dimethylsiloxane) (PDMS) elastomer stamps through hydrophobic interactions and the transfer of these monolayers onto gold surfaces in μCP is a classical example of such an affinity printing method.[10,11] When used in conjunction with chemically patterned and topographically flat stamps, these methods can afford excellent printing resolutions.[16] The concept of printing has recently been extended from molecular monolayers to nanoparticulate monolayers.[17–22] Nanoparticles, synthesized through controlled wet-chemical synthesis routes, bear exciting optical, electronic, and magnetic properties often superior to those of lithographically defined nanostructures.[23,24] Methods that allow the integration of these nanoparticle building blocks into functional devices are of pivotal importance for the exploitation of their unique properties. The ability to accurately place individual nanoparticles onto large surface areas will be a key requirement towards their advanced applications such as plasmonic structures for biosensors,[25] photovoltaic applications,[26] and optoelectronic circuits.[27] Although several concepts have been introduced to produce nanoparticle patterns by printing techniques,[17–22] very few of those studies demonstrate the feasibility of printing single nanoparticle arrays[21,22] and those that do, provide limited variability of the pattern design or the reusability of the nanopatterned stamps for multiple printing cycles was not tested.

Herein, we present a novel affinity-based Gutenberg-style nanoprinting approach for the production of custom-defined nanoparticle assemblies through a repetitive printing process. Electrostatic nanoparticle assembly and DNA-mediated nanoparticle transfer are used to replicate nanostructures fabricated by electron-beam lithography (EBL). Furthermore, the potential of printing nanofeatures with single-nanoparticle resolution were explored and the nanoparticle assembly and transfer efficiencies in repetitive printing cycles were quantified.

A variety of print masters, consisting of gold nanopatterns on silica-coated silicon (100) wafers, were produced to serve as stamps. These were fabricated by a sequence of EBL, wet-chemical etching, metal deposition, and lift-off processes. Self-assembled monolayers were adsorbed onto the surface of these print masters by exploiting the selective affinity of silanes and thiols to silica and gold. First, polyethylene glycol (PEG)-silane (see Scheme 1c) was used to passivate the silica surface through a condensation reaction to block nonspecific nanoparticle adsorption. Following the PEG-silane treatment, a monolayer of SH-PEG-NH_2·HCl (see Scheme 1c) was deposited onto the exposed gold surfaces by gold–thiol functionalization. Gold nanoparticles (40 nm diameter), capped with a layer of negatively charged DNA strands (DNA-AuNPs), were used as nanoparticle building blocks.

The principle of DNA-mediated Gutenberg-style nanoprinting is illustrated in Scheme 1a. A freshly prepared print master (stamp) was exposed to a solution of DNA-AuNPs in a buffered saline solution to allow for the electrostatic assembly of the nanoparticles (step ①). Following the self-assembly step, the stamp was removed from the DNA-AuNP solution,

[*] Y. H. Zheng, T. Thai, Dr. U. Bach
Department of Materials Engineering, Monash University
Wellington RD, Clayton, Victoria 3800 (Australia)
Fax: (+61) 3-990-56264
E-mail: udo.bach@sci.monash.edu.au
C. H. Lalander, Dr. U. Bach
School of Chemistry, Monash University (Australia)
Dr. S. Dhuey, Dr. S. Cabrini
Molecular Foundry, Lawrence Berkeley National Laboratories (LBNL)
1 Cyclotron Road, Berkeley, CA 94720 (USA)

[**] This project was supported by the Australian Research Council (DP0665223, LE0883019) and the Lawrence Berkeley National Laboratories (Molecular Foundry, user projects 187, 440, 1064). Dr. S. Watkins (CSIRO) and Dr. B. Harteneck (LBNL) are acknowledged for their experimental assistance. The Monash Center for Electron Microscopy is acknowledged for the use of their facilities and the provision of scientific and technical assistance. Finally, we would like to thank Inga Tegtmeier (Advanced Design and Communication) for providing valuable graphic design expertise.

Supporting information for this article is available on the WWW under http://dx.doi.org/10.1002/anie.201006991.

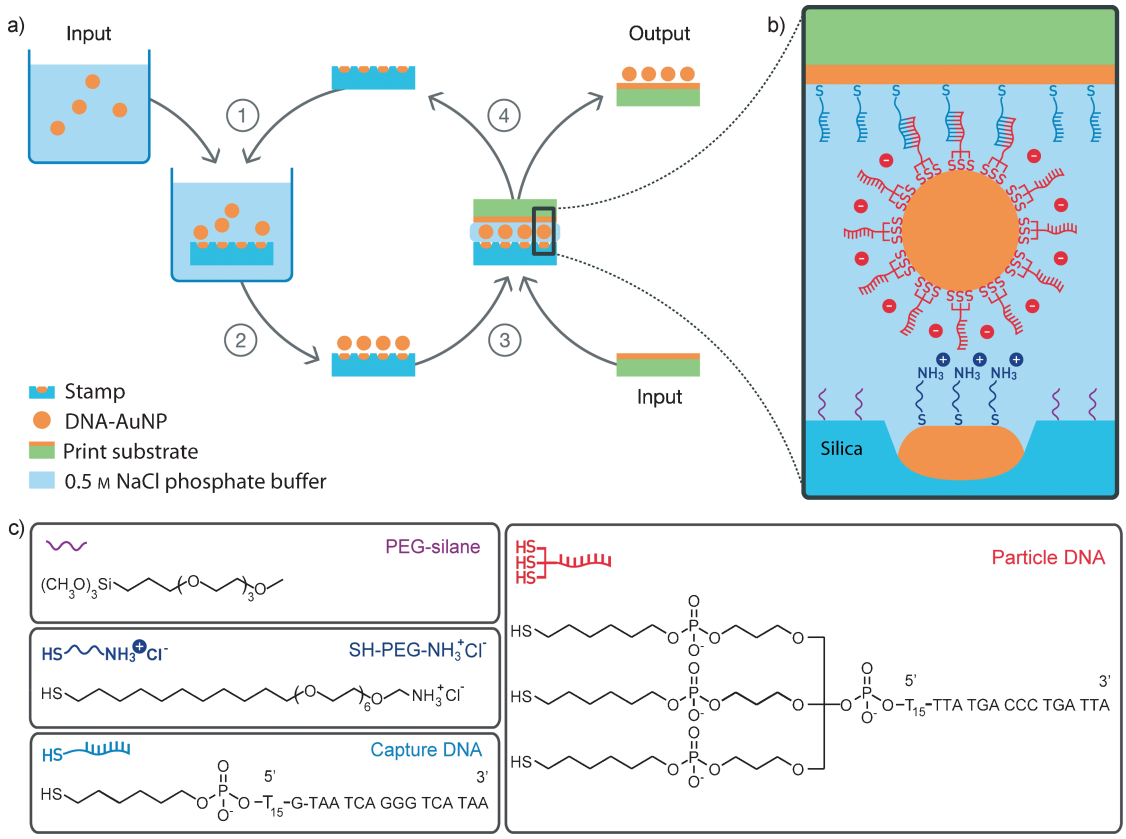

Scheme 1. a) Outline of the printing process: ① A gold-on-silicon nanopattern (master) is exposed to a solution of DNA-AuNPs to allow for their electrostatic adsorption. ② The print master is removed from the DNA-AuNP solution, washed, and dried. ③ To transfer the assembled nanoparticles, the print master and print substrate are brought into close contact in the presence of a buffer and controlled pressure is applied. ④ The pressure is released and the two substrates are separated from each other, yielding a DNA-AuNP array on the print substrate which replicates the nanopattern on the print master. The print master is regenerated for the subsequent printing cycle. b) Cross-section diagram of a DNA-AuNP located between the print master and print substrate during the printing step. The silica surface of the print master is passivated through a condensation reaction with PEG-silane. The negatively charged DNA-AuNPs self-assemble onto the gold surface of the print master, to which a self-assembled monolayer of SH-PEG-NH_2·HCl confers a positive surface charge. During the printing process the complementary DNA strands located on the nanoparticle (particle DNA) and print substrate (capture DNA) hybridize, binding the nanoparticle to the print substrate. c) Chemical structures of surface-active compounds and DNA sequences.

washed with ultrapure water, and dried in air (step ②). To transfer the self-assembled AuNPs, the stamp was brought into close contact with a gold-coated silicon (100) wafer (print substrate), modified with complementary capture DNA, and a pressure of 10 N cm^{-2} was applied in the presence of a buffer (step ③), allowing the particle DNA to hybridize with the capture DNA on the print substrate (Scheme 1b). Subsequently, the pressure was released, yielding the print substrate carrying a nanoparticle replica of the original EBL surface nanopattern (step ④). The master was prepared for the subsequent printing step through a sequence of UV–ozone, PEG-silane, and SH-PEG-NH_2·HCl treatments. A detailed description of all fabrication, nanoparticle assembly, and printing processes is provided in the Supporting Information.

Two test nanopatterns were used to study the self-assembly and printing process described in Scheme 1. Pattern A consists of a periodic array of lithographically defined gold nanowires (Figure 1a). Single rows of DNA-AuNPs specifically assemble on the top of these elevated gold nanofeatures (Figure 1b). This is attributed to the electrostatic attraction[28,29] between the negatively charged DNA-AuNPs[30] and the gold surface nanopatterns, to which the self-assembled monolayer of SH-PEG-NH_2·HCl confers a net positive surface charge.[31] The atomic force microscope (AFM) image shows that less than 1% of the immobilized DNA-AuNPs adsorb to the sides of the nanowires or onto the surrounding PEGylated silica surface. This can be rationalized in terms of a net negative surface charge, confined to the surrounding silica surfaces at neutral pH,[32] directing the self-assembly of the DNA-AuNPs onto the center of the elevated gold nanowires and away from the silica surface.[33] Figure 1c shows the successfully transferred DNA-AuNP lines, as well as the typical grainy structure of the underlying evaporated gold layer. The original line structure of the master substrate is well replicated. The efficiency of transferring assembled nanoparticles was calculated to be 89%. Pattern B consists of a recessed gold nanostructure with negative surface features in the shape of a linear array of six gold dots (Figure 1d). This was obtained by introducing a wet-chemical etching step to the master fabrication process (see the Supporting Informa-

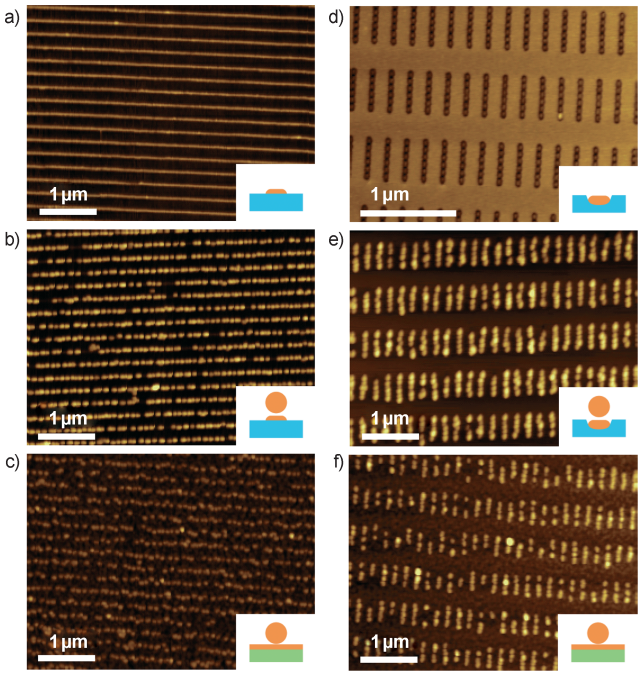

Figure 1. Gutenberg-style printing of metal nanoparticle arrays. AFM images of stamps before and after nanoparticle loading as well as the printed nanoparticle arrays: a) Pattern A consisting of lithographically defined gold nanowires deposited onto the flat surface of a silica-coated wafer (nanowire height 6–8 nm, width 32 nm, length 20 μm, spacing 200 nm; patterned area: 100 μm × 100 μm). b) Pattern A after DNA-AuNP assembly from solution. c) Printed DNA-AuNP array imaged on the print substrate, replicating the geometry of nanopattern A. d) Pattern B consisting of linear groupings of six slightly recessed gold dots ("six-dot-line") on a silica-coated silicon wafer (size of each dot: 36 nm, center-to-center distance of two adjacent dots (pitch): 55 nm, patterned area: 1×1 mm^2). Each metal dot is deposited into a small depression, fabricated by a wet-chemical etching step. This results in a nanopattern that is topographically slightly recessed (the top of the gold dots is located 2–5 nm below the wafer surface). e) Pattern B after DNA-AuNP assembly from solution. f) Printed DNA-AuNP array on the print substrate, replicating pattern B. See the Supporting Information for more details on the stamp fabrication, self-assembly, and printing process.

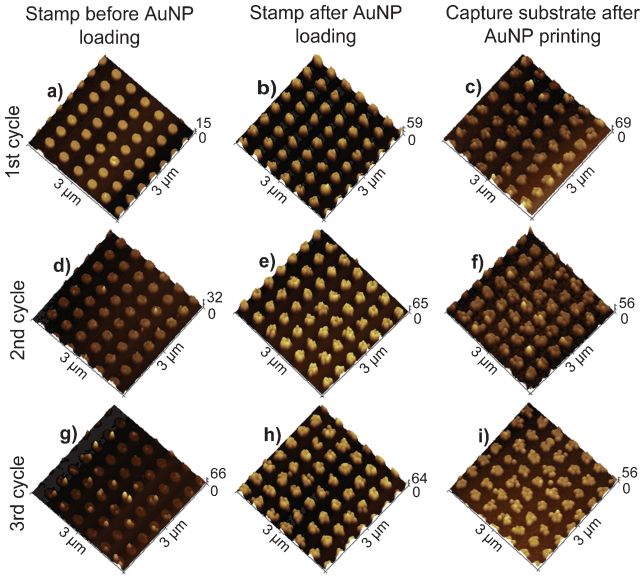

Figure 2. Representative AFM images of stamp and print substrates over three consecutive print cycles. A stamp consisting of a silicon wafer with a 110 nm thick silicon oxide layer, coated with a regular array of gold nanodisks with a thickness and a diameter of 8 and 200 nm, was used to validate the cyclic repeatability of the printing process shown in Scheme 1. For three consecutive print cycles AFM images of the stamp prior to (a, d, g) and following (b, e, h) DNA-AuNP loading are shown. Panel c), f), and i) show the printed nanopattern on the print substrates resulting from each of the three printing cycles. The center-to-center distance of adjacent gold disks is 400 nm.

tion). The etching depth was chosen to be two to five nanometers greater than the thickness of the subsequently evaporated metal layers to produce slightly recessed gold sites. This test structure was developed with the aim to design adsorption sites that are tailored towards the adsorption of individual nanoparticles in close vicinity to each other.[34] The latter is crucial for a number of potential applications such as plasmonic circuits that rely on the optical or electronic interaction of neighboring nanoparticles. Figure 1e shows an AFM micrograph of DNA-AuNPs assembled onto the positively charged six-dot-line gold nanopatterns. The nanoparticles produce a good replicate of the underlying template structure, with an average of 5.0 particles assembled in a linear fashion onto each pattern. This could indicate that the pitch of 55 nm chosen for the six-dot-line gold nanopattern was slightly too small to accommodate the adsorption of six nanoparticles.[34] Figure 1f shows the printed pattern of the AuNPs on the replica substrate, featuring an average of 3.8 nanoparticles per six-dot-line structures, corresponding to a transfer yield of 76%. A similar transfer efficiency was observed over the entire 1×1 mm^2 area of the nanopattern, consisting of more than thirty million individual adsorption sites (see Figure S1 in the Supporting Information).

To validate the cyclic repeatability of the printing process, a stamp that consists of a regular array of lithographically defined gold nanodisks on a SiO_2/Si(100) wafer (Pattern C, see Figure 2a) was used continuously for a total of three consecutive printing cycles. Representative AFM images and a statistical analysis of the assembly and transfer yields are shown in Figures 2 and 3. An AFM image of the stamp following the surface functionalization with SH-PEG-NH_2·HCl and the subsequent immobilization of DNA-AuNPs is shown in Figure 2b. The DNA-AuNPs specifically adsorbed onto the functionalized gold surface, forming a densely packed monolayer. Statistical analysis revealed that an average of 9.9 AuNPs adsorbed onto each gold nanodisk. Figure 2c shows the nanoparticle pattern after its successful transfer to a print substrate. An average of 8.9 particles per pattern were transferred during the printing process. The stamp was then regenerated for the following printing cycle by a subsequent dummy print, and UV–ozone, PEG-silane, and SH-PEG-NH_2·HCl treatments. The UV–ozone treatment was vital for achieving high particle loadings in the subsequent self-assembly step (see Figure S2 in the Supporting Information). The AFM images for the second and third printing cycle (Figure 2d–i), along with the statistical data

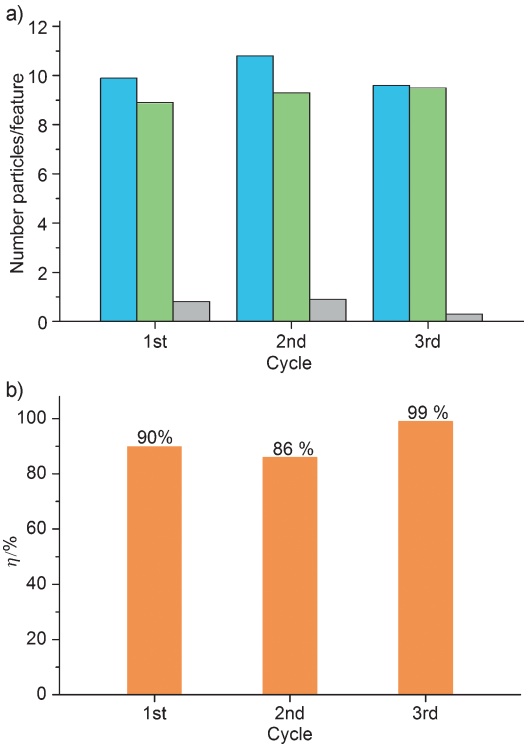

Figure 3. Nanoparticle loading and transfer yield (η). a) For each of the three consecutive print cycles, the average number of self-assembled (blue) and transferred (green) DNA-AuNPs for each gold nanodisk was analyzed. The number of DNA-AuNPs remaining on the stamp immediately after the printing process (gray) is also shown (AFM images, see Figure S3 in the Supporting Information). b) Calculated transfer yield for DNA-AuNPs from the stamp to the print substrate for each of the three printing cycles.

shown in Figure 3, reveal similar assembly and transfer yields to the first printing cycle. Closely packed nanoparticle loading and transfer efficiencies of 90, 86, and 99 %, respectively, were observed for all three print cycles. Nonspecific adsorption of the DNA-AuNPs onto the silica surface remained insignificant over the three cycles. An average of less than one nanoparticle per gold nanodisk remained on the stamp after each printing cycle (see Figure S3 in the Supporting Information). The transfer efficiency was much lower when print substrates, modified with noncomplementary layers of DNA, were used with an average of 5.0 DNA-AuNPs remaining on each gold nanodisk after the printing process (see Figure S4 in the Supporting Information). This confirmed that the specific interaction of DNA strands between the assembled DNA-AuNPs and the print substrate was essential to obtain high transfer yields.

In conclusion, we have demonstrated the feasibility of a novel affinity-based Gutenberg-style nanoprinting strategy that uses chemically modified surfaces for the selective adsorption and transfer of nanoparticles from a lithographically patterned master to a print substrate. Printing of 40 nm gold nanoparticles from recessed and elevated nanostructures was successfully demonstrated. Single lines of nanoparticles and regular nanoparticle patterns with close to single-particle resolution could be printed. These results are unmatched by conventional μCP techniques which are limited to feature sizes of around 150 nm as a consequence of the mechanical properties of the elastomeric stamp and ink diffusion issues.[13,35] The use of topographically flat print masters and the exploitation of inking and ink-transfer processes based on self-assembly and molecular recognition are mainly responsible for the improvement in printing resolution. High nanoparticle loading and high transfer yields were observed over three consecutive printing cycles, proving the potential to use lithographically fabricated masters in continuous printing processes. The integrity of the printed gold nanoparticle assemblies was not affected by either storage over several months or treatment with UV–ozone for 30 min, which was shown to remove the monolayer of surface-confined DNA molecules (see Figure S5 in the Supporting Information). The latter could make these patterns applicable to a wider range of applications such as plasmonic biosensors that require pristine metal nanoparticle arrays.[25]

This new pattern replication strategy combines the high-resolution advantage of direct-write nanolithography techniques with 1) the low-cost and high-throughput advantages of nanoprinting techniques, 2) the programmability of DNA-directed pattern transfer, and 3) the extraordinary materials properties of chemically synthesized nanomaterials, into one nanofabrication process. A number of challenges still lie ahead, before nanoparticle printing techniques like that described here can be exploited for the mass fabrication of functional devices such as solar cells, plasmonic circuits, and biosensors. Currently stamp regeneration between each printing cycle is necessary to maintain high printing fidelity over repetitive print cycles. We are currently exploring alternative printing strategies based on flexible print substrates. This should make it possible to achieve conformal contact of stamp and print substrate at significantly reduced pressures and reduce the impact of the printing process on the integrity of the self-assembled monolayers (SAMs) pattern of the stamp. Further optimization of the geometry of the single-particle adsorption sites (Figure 1 d), the mechanical property of the stamp, the functionality of the surface, and particle-confined SAMs are currently in progress, targeting the rapid, quantitative assembly and transfer of single-nanoparticle features over a large number of printing cycles. The concept introduced here can be extended further by exploiting specific DNA–DNA interactions rather than electrostatic interaction for the assembly of nanoparticles onto the stamp. While this would require careful balancing of the hybridization energetics that prevail during nanoparticle loading and transfer, it would also provide the full benefit of DNA-directed self-assembly with its associated unlimited programmability of nanoparticle loading and transfer.

Received: November 8, 2010
Revised: February 17, 2011
Published online: April 7, 2011

Keywords: DNA · nanoparticles · nanopatterns · nanoprinting · self-assembly

[1] I. Sychugov, Y. Nakayama, K. Mitsuishi, *Nanotechnology* **2010**, *21*, 285307.
[2] J. S. Wi, T. Y. Lee, H. M. Kim, H. S. Lee, S. W. Nam, I. J. Shin, K. H. Shin, K. B. Kim, *Adv. Mater.* **2007**, *19*, 3469 – 3472.
[3] F. Lehmann, G. Richter, T. Borzenko, V. Hock, G. Schmidt, L. W. Molenkamp, *Microelectron. Eng.* **2003**, *65*, 327 – 333.
[4] W. K. Lee, S. Chen, A. Chilkoti, S. Zauscher, *Small* **2007**, *3*, 249 – 254.
[5] M. Rolandi, C. F. Quate, H. Dai, *Adv. Mater.* **2002**, *14*, 191 – 194.
[6] H. Sugimura, T. Hanji, K. Hayashi, O. Takai, *Adv. Mater.* **2002**, *14*, 524 – 526.
[7] D. Wang, V. K. Kodali, W. D. Underwood II, J. E. Jarvholm, T. Okada, S. C. Jones, M. Rumi, Z. Dai, W. P. King, S. R. Marder, J. E. Curtis, E. Riedo, *Adv. Funct. Mater.* **2009**, *19*, 3696 – 3702.
[8] R. Szoszkiewicz, T. Okada, S. C. Jones, T. D. Li, W. P. King, S. R. Marder, E. Riedo, *Nano Lett.* **2007**, *7*, 1064 – 1069.
[9] J. Lee, T. Beechem, T. L. Wright, B. A. Nelson, S. Graham, W. P. King, *J. Microelectromech. Syst.* **2006**, *15*, 1644 – 1655.
[10] Y. Xia, E. Kim, M. Mrksich, G. M. Whitesides, *Chem. Mater.* **1996**, *8*, 601 – 603.
[11] L. Libioulle, A. Bietsch, H. Schmid, B. Michel, E. Delamarche, *Langmuir* **1999**, *15*, 300 – 304.
[12] C. Pina-Hernandez, L. J. Guo, P. F. Fu, *ACS Nano* **2010**, *4*, 4776 – 4784.
[13] M. H. Lee, J. Y. Lin, T. W. Odom, *Angew. Chem.* **2010**, *122*, 3121 – 3124; *Angew. Chem. Int. Ed.* **2010**, *49*, 3057 – 3060.
[14] A. Bernard, D. Fitzli, P. Sonderegger, E. Delamarche, B. Michel, H. R. Bosshard, H. Biebuyck, *Nat. Biotechnol.* **2001**, *19*, 866 – 869.
[15] H. Lin, L. Sun, R. M. Crooks, *J. Am. Chem. Soc.* **2005**, *127*, 11210 – 11211.
[16] Z. Zheng, J. W. Jang, G. Zheng, C. A. Mirkin, *Angew. Chem.* **2008**, *120*, 10099 – 10102; *Angew. Chem. Int. Ed.* **2008**, *47*, 9951 – 9954.
[17] R. Klajn, K. J. M. Bishop, M. Fialkowski, M. Paszewski, C. J. Campbell, T. P. Gray, B. A. Grzybowski, *Science* **2007**, *316*, 261 – 264.
[18] V. Santhanam, R. P. Andres, *Nano Lett.* **2004**, *4*, 41 – 44.
[19] L. Kim, P. O. Anikeeva, S. A. Coe-Sullivan, J. S. Steckel, M. G. Bawendi, V. Bulović, *Nano Lett.* **2008**, *8*, 4513 – 4517.
[20] W. Cheng, N. Park, M. T. Walter, M. R. Hartman, D. Luo, *Nat. Nanotechnol.* **2008**, *3*, 682 – 690.
[21] N. Pazos-Pérez, W. Ni, A. Schweikart, R. A. Alvarez-Puebla, A. Fery, L. M. Liz-Marzan, *Chem. Sci.* **2010**, *1*, 174 – 178.
[22] T. Kraus, L. Malaquin, H. Schmid, W. Riess, N. D. Spencer, H. Wolf, *Nat. Nanotechnol.* **2007**, *2*, 570 – 576.
[23] H. Ditlbacher, A. Hohenau, D. Wagner, U. Kreibig, M. Rogers, F. Hofer, F. R. Aussenegg, J. R. Krenn, *Phys. Rev. Lett.* **2005**, *95*, 257403.
[24] T. Laroche, A. Vial, M. Roussey, *Appl. Phys. Lett.* **2007**, *91*, 123101.
[25] J. N. Anker, W. P. Hall, O. Lyandres, N. C. Shah, J. Zhao, R. P. Van Duyne, *Nat. Mater.* **2008**, *7*, 442 – 453.
[26] H. A. Atwater, A. Polman, *Nat. Mater.* **2010**, *9*, 205 – 213.
[27] E. Ozbay, *Science* **2006**, *311*, 189 – 193.
[28] C. S. Chiu, H. M. Lee, C. T. Kuo, S. Gwo, *Appl. Phys. Lett.* **2008**, *93*, 163106.
[29] K. Bandyopadhyay, E. Tan, L. Ho, S. Bundick, S. M. Baker, A. Niemz, *Langmuir* **2006**, *22*, 4978 – 4984.
[30] W. J. Parak, T. Pellegrino, C. M. Micheel, D. Gerion, S. C. Williams, A. P. Alivisatos, *Nano Lett.* **2003**, *3*, 33 – 36.
[31] M. Hanauer, S. Pierrat, I. Zins, A. Lotz, C. Sönnichsen, *Nano Lett.* **2007**, *7*, 2881 – 2885.
[32] K. Rezwan, L. P. Meier, L. J. Gauckler, *Biomaterials* **2005**, *26*, 4351 – 4357.
[33] L. C. Ma, R. Subramanian, H. W. Huang, V. Ray, C. U. Kim, S. J. Koh, *Nano Lett.* **2007**, *7*, 439 – 445.
[34] C. H. Lalander, Y. Zheng, S. Dhuey, S. Cabrini, U. Bach, *ACS Nano* **2010**, *4*, 6153 – 6161.
[35] M. Geissler, H. Wolf, R. Stutz, E. Delamarche, U. W. Grummt, B. Michel, A. Bietsch, *Langmuir* **2003**, *19*, 6301 – 6311.

